



Contents lists available at ScienceDirect

# Journal of Quantitative Spectroscopy & Radiative Transfer

journal homepage: [www.elsevier.com/locate/jqsrt](http://www.elsevier.com/locate/jqsrt)

## Measured integrated band intensities and simulated line-by-line spectra for $^{12}\text{C}_2\text{HD}$ between 25 and 2.5 $\mu\text{m}$ , and new global vibration–rotation parameters for the bending vibrations

A. Jolly<sup>a,\*</sup>, Y. Benilan<sup>a</sup>, E. Cané<sup>b</sup>, L. Fusina<sup>b</sup>, F. Tamassia<sup>b</sup>, A. Fayt<sup>c</sup>, S. Robert<sup>d,1</sup>, M. Herman<sup>d</sup><sup>a</sup> Laboratoire Interuniversitaire des Systèmes Atmosphériques, UMR 7583 du CNRS, Universités Paris XII—Val de Marne et Paris VII, 61 Av. Général de Gaulle, F-94010 Créteil Cedex, France<sup>b</sup> Dipartimento di Chimica Fisica e Inorganica, Università di Bologna, Viale del Risorgimento, 4, I-40136 Bologna, Italy<sup>c</sup> Laboratoire de Spectroscopie Moléculaire, Université Catholique de Louvain, Chemin du Cyclotron, 2, B-1348 Louvain-La-Neuve, Belgium<sup>d</sup> Service de Chimie quantique et Photophysique CP 160/09, Faculté des Sciences, Université Libre de Bruxelles (U.L.B.), Av. Roosevelt, 50, B-1050 Bruxelles, Belgium

### ARTICLE INFO

#### Article history:

Received 2 July 2008

Received in revised form

11 August 2008

Accepted 17 August 2008

#### Keywords:

Titan's atmosphere

 $^{12}\text{C}_2\text{HD}$ 

Bending vibrations

Global analysis

Integrated band intensities

### ABSTRACT

The global analysis of published high-resolution vibration–rotation spectra of  $^{12}\text{C}_2\text{HD}$  in the bending spectral range is presented, resulting in an extension of the known vibration–rotation assignments, including a new band  $2\nu_4+\nu_5\leftarrow 2\nu_4$  ( $1^1I\leftarrow 1^1A$ ). Experimental integrated band intensities are reported in the range from 25 to 2.5  $\mu\text{m}$ , and both  $\nu_4$  and  $\nu_5$  bending fundamentals are simulated line by line. An extensive line list is produced in the bending energy range, to supply previously missing information in databases.

© 2008 Elsevier Ltd. All rights reserved.

### 1. Introduction

Monodeuterated acetylene,  $^{12}\text{C}_2\text{HD}$ , was detected in Titan's atmosphere [1] in the thermal infrared at a spectral resolution of  $0.5\text{ cm}^{-1}$  by the CIRS instrument mounted on CASSINI spacecraft. This is the first detection of  $\text{C}_2\text{HD}$  in an astronomical environment. This isotopologue of acetylene has been identified through its strongest bending mode  $\nu_5$  at  $677.8\text{ cm}^{-1}$  and confirmed by the observation of a small feature at  $518.4\text{ cm}^{-1}$  corresponding to the weaker bending mode  $\nu_4$ . Both  $\nu_4$  and  $\nu_5$  bands show sharp Q branches, which are the strongest spectral features of this species in this spectral range [2]. The molecule has a very small dipole moment and its rotational spectrum has been observed only in the laboratory [3].

Many spectral investigations have been devoted to  $^{12}\text{C}_2\text{HD}$  (e.g. [3–8]). High-resolution studies have provided a very good characterization of the vibration–rotation spectrum of many bands but none of them have dealt with intensities. Only two different research groups have measured integrated intensities of the fundamental bands recorded at low resolution using impure samples [9,10]. Finally, no intensity line list was available at the time of detection to help quantify the amount of  $^{12}\text{C}_2\text{HD}$  present in Titan's atmosphere.

\* Corresponding author.

E-mail address: [jolly@lisa.univ-paris12.fr](mailto:jolly@lisa.univ-paris12.fr) (A. Jolly).<sup>1</sup> FRIA researcher.

In Section 2, we present new results achieved in Paris on the measurement of integrated intensities of the main bands of  $^{12}\text{C}_2\text{HD}$  between 1000 and 4000  $\text{cm}^{-1}$ , using a 97% pure sample, and compare our results to earlier studies. Previous intensity measurements concerning the  $\nu_4$  and  $\nu_5$  fundamental bands have already been used in the quantification of  $^{12}\text{C}_2\text{HD}$  in Titan's atmosphere [1].

In Section 3, we propose a re-analysis performed in Brussels of the line positions in the high-resolution spectra of both bending modes recorded in Bologna using global analysis programs developed at Louvain la Neuve.

In Section 4, before concluding in Section 5, we use the package of computer programs just mentioned to perform spectra simulation, thus focusing on line intensities. The simulations are scaled using the newly measured integrated band intensities reported in Section 2. A new line list is produced, limited to the spectral range of the bending bands. It includes 7000 lines and will be made available in the next update of the GEISA database.

The usual normal-mode vibrational numbering in acetylene is used throughout the paper, namely  $\nu_1$  and  $\nu_3$  for the symmetric ( $\sigma^+$ ) and antisymmetric ( $\sigma^+$ ) CH stretchings, respectively,  $\nu_2$  for the CC stretching ( $\sigma^+$ ), and  $\nu_4$  and  $\nu_5$  for the degenerate *trans* ( $\pi$ ) and *cis* ( $\pi$ ) bendings, respectively. A pronounced local-mode character is known to arise in  $^{12}\text{C}_2\text{HD}$ , with  $\nu_1$  being the CH stretching,  $\nu_3$  the CD stretching,  $\nu_4$  the CD bending and  $\nu_5$  the CH bending.

## 2. Absolute intensity measurements

Eggers et al. [9] measured for the first time the integrated intensities of all fundamental bands of  $^{12}\text{C}_2\text{HD}$ ,  $^{12}\text{C}_2\text{H}_2$  and  $^{12}\text{C}_2\text{D}_2$ . They estimate the uncertainty of their measurements to be about 20% for both  $\nu_4$  and  $\nu_5$  bending bands, 10% for both strong  $\nu_1$  and  $\nu_3$  stretching bands and over 50% for the very weak  $\nu_2$  band. Later, Kim and King [10] obtained new intensity values for the same isotopologues. All five fundamental bands of  $^{12}\text{C}_2\text{HD}$  were measured and the uncertainties were estimated to be between 3% and 5%. In both studies, the  $\text{C}_2\text{HD}$  sample has been synthesized by the authors with limited isotopic purity. Eggers et al. [9] estimated a relative amount of 66% of  $^{12}\text{C}_2\text{HD}$  in their sample by mass spectrometry. Kim and King [10] obtained 61.5%,  $\text{C}_2\text{H}_2$  and  $\text{C}_2\text{D}_2$  being the other constituents with 29.5% of  $\text{C}_2\text{H}_2$ . As can be seen in Table 1, the integrated intensities are systematically larger in Kim and King's study. A good agreement is obtained for the  $\nu_4$  band, but the discrepancy reaches 27% for the strong  $\nu_5$  band and about 15% for the stretching bands  $\nu_1$  and  $\nu_3$ . Similarly, for  $^{12}\text{C}_2\text{D}_2$ , their values are 15–20% larger than those of Eggers. These discrepancies are surprising, considering that a very good agreement (2%) was obtained for the two active (u/g allowed) fundamental bands,  $\nu_3$  and  $\nu_5$ , of  $^{12}\text{C}_2\text{H}_2$ .

Errors in the estimate of the concentration of  $^{12}\text{C}_2\text{HD}$  and  $^{12}\text{C}_2\text{D}_2$  in the samples could be responsible for the observed discrepancies. Another source of error could be the overlap of  $\text{C}_2\text{HD}$  and  $\text{C}_2\text{H}_2$  bands. In Kim and King's measurement, the amount of  $\text{C}_2\text{H}_2$  and the strength of the  $\nu_5$  band, indeed, lead to a peak at 729  $\text{cm}^{-1}$  with almost the same intensity as the  $\text{C}_2\text{HD}$  peak at 678  $\text{cm}^{-1}$ , and consequently to a strong overlap between both contributions.

In our experiment, a 25-cm-long multipass cell was used to measure absorption spectra of  $\text{C}_2\text{HD}$  at room temperature (296 K) using a Bruker Equinox 55 FTIR spectrometer at 0.5  $\text{cm}^{-1}$  resolution. We use a KBr beamsplitter and a DTGS D301 detector, which has a linear response from 400 to 5000  $\text{cm}^{-1}$ . The optical path was set to 1060 cm and the pressure ranged from 0.01 to 0.05 mbar. Acetylene-d1 was purchased from C/D/N Isotopes Inc. The enrichment measured by gas chromatography and mass spectrometry was 97%. For eight different pressures, spectra of the mixture of the sample with about 1000 mbar of nitrogen were recorded. To obtain a signal-to-noise ratio of 1000, 200 scans were added for each spectrum. An overview of the spectra in the 1000–4000  $\text{cm}^{-1}$  range is presented in Fig. 1.

Our results are listed in Table 1. In addition to the five fundamental bands, integrated intensities of two overtone and three combination bands are presented. The tabulated values and uncertainties are derived for each band from the average and the standard deviation of the measured integrated band coefficients from five to six different spectra. Selected

**Table 1**

Position and absolute intensity of the vibrational bands of  $^{12}\text{C}_2\text{HD}$  between 10 and 2.5  $\mu\text{m}$

Band	$G_v^0$ ( $\text{cm}^{-1}$ ) <sup>a</sup>	Absolute intensity ( $\text{cm}^{-2} \text{atm}^{-1}$ ) at 296 K		
		This work	Eggers et al. [9]	Kim and King [10]
$\nu_1+\nu_5$	3996.0	1.0 ± 0.1	–	–
$\nu_1$	3335.61	103.6 ± 3	100.7 ± 20	124 ± 4
$\nu_3+\nu_4$	3086.65	0.29 ± 0.1	–	–
$\nu_3$	2583.60	73.5 ± 2	77 ± 13	89.4 ± 2
$\nu_2$	1853.78	3.1 ± 1	2.6 ± 1.5	4.1 ± 1
$2\nu_5$	1342.23	30.7 ± 2	–	–
$\nu_4+\nu_5$	1200.50	5.8 ± 0.5	–	–
$2\nu_4$	1033.93	14.2 ± 2	–	–
$\nu_5$	678.80	354.7 ± 9	343.6 ± 68	472.9 ± 9
$\nu_4$	519.38	73.2 ± 3	80.3 ± 16	82.4 ± 1.6

<sup>a</sup> Values as reported in Ref. [7].

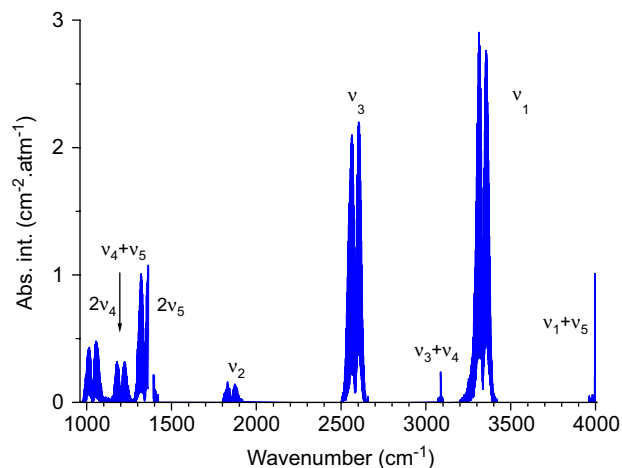


**Fig. 1.** Overview of the spectral range between 1000 and 4000  $\text{cm}^{-1}$  in  $^{12}\text{C}_2\text{HD}$  ( $T = 296\text{ K}$ , pathlength = 10.6 m,  $P = 0.0245\text{ mbar}$ , resolution =  $0.5\text{ cm}^{-1}$ ).

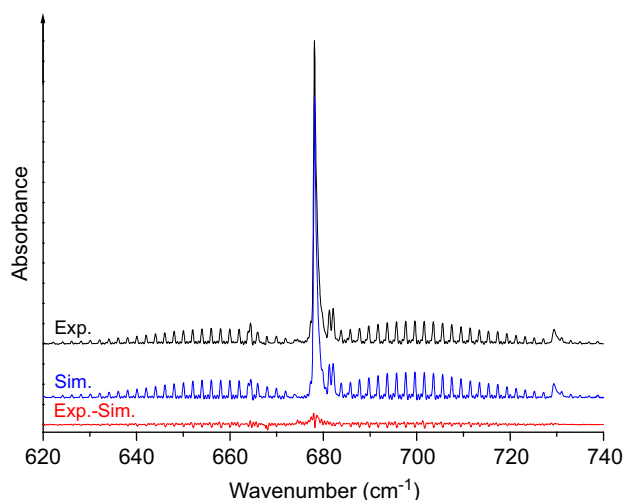


**Fig. 2.** Comparison between simulated and experimental spectra near the  $\nu_5$  bending of  $^{12}\text{C}_2\text{HD}$  ( $T = 296\text{ K}$ , pathlength = 10.6 m,  $P = 0.155\text{ mbar}$ , resolution =  $0.5\text{ cm}^{-1}$ ). The spectral feature around  $729\text{ cm}^{-1}$  is the Q-branch of  $\nu_5$ ,  $^{12}\text{C}_2\text{H}_2$ . The simulation was done assuming 3% of  $^{12}\text{C}_2\text{H}_2$  in the sample.

low-pressure spectra were not included in the calculation of the band intensities of the weak bands. Similarly, spectra above 0.034 mbar were not considered for the strong  $\nu_5$  band, because saturation of the Q branch was observed. Our uncertainties do not exceed 5% for the fundamental bands except for  $\nu_2$ , where the weakness of the band and overlaps with residual water lines make the measurement very uncertain. The agreement between the present and Eggers' results is very good. On the contrary, the disagreement with Kim and King's results reaches 24% for the strong  $\nu_5$  band and is about 15% for the other bands, except for the very weak  $\nu_2$  band.

As can be seen in Fig. 2, the presence of  $^{12}\text{C}_2\text{H}_2$  in the sample used is clearly observed at  $729\text{ cm}^{-1}$ . The value of 3% of acetylene has been estimated by the calculations of synthetic spectra for both bands. Given a 97% pure sample and a resolution good enough to avoid almost any overlap, the present results are expected to be more reliable than the previous ones.

### 3. High-resolution spectra analysis

The high-resolution spectra were recorded in Bologna at room temperature in the region between 450 and 2100  $\text{cm}^{-1}$  using a BOMEM DA3.002 FT interferometer equipped with a KBr beamsplitter, Globar source and two different HgCdTe detectors [2]. The absorption pathlength varied from 0.18 to 7.0 m and the sample pressure from 30 to 1300 Pa. The

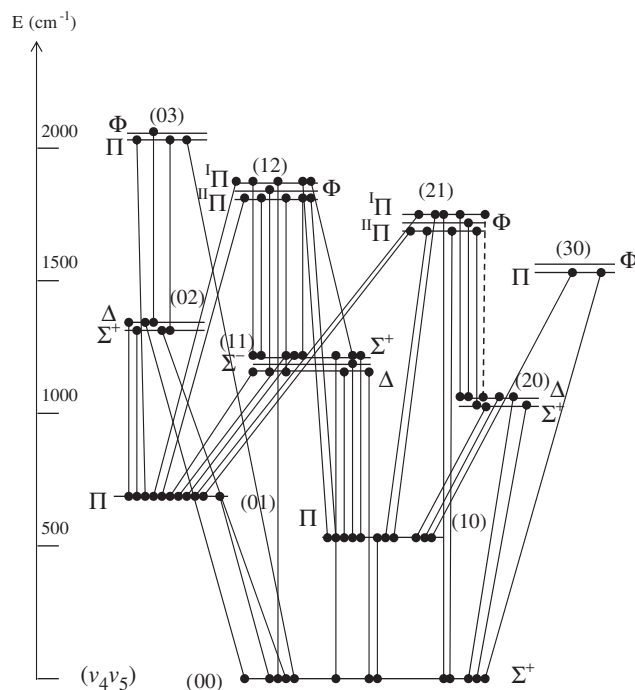


**Fig. 3.** Vibrational states and transitions in  $^{12}\text{C}_2\text{HD}$  taken into account in the present investigation, with the following labels: (—) from Ref. [2] and (---) presently newly assigned. The states are identified with the values of the bending vibrational quantum numbers  $(v_4, v_5)$ .

resolution ranged from  $0.004$  to  $0.006 \text{ cm}^{-1}$ . Ro-vibrational transitions of  $\text{H}_2\text{O}$  and  $\text{CO}_2$  were used for calibration. Additional experimental details can be found in Ref. [2]. All vibrational transitions connecting bending states available in the literature and used for the global fit are shown in Fig. 3.

A global Hamiltonian can account for all terms relevant to the simultaneous fit of all vibration–rotation lines up to highly excited vibrational ranges in linear molecules, as demonstrated up to  $6750 \text{ cm}^{-1}$  for  $^{13}\text{CH}^{12}\text{CH}$  [11]. Global fits were actually applied to the more limited bending energy range in a number of acetylene isotopologues, namely  $^{12}\text{C}_2\text{H}_2$  [12,13],  $^{12}\text{C}_2\text{D}_2$  [14],  $^{13}\text{C}_2\text{D}_2$  [15],  $^{13}\text{CH}^{12}\text{CH}$  [16] and also  $^{12}\text{C}_2\text{HD}$  [2]. We have achieved a new global fit in  $^{12}\text{C}_2\text{HD}$ , now using a computer package developed in Louvain-La-Neuve and dedicated to both energy and intensity treatments [17,18]. The matrix elements in the Hamiltonian used to perform this global vibration–rotation fit are detailed in Table 2. As pointed out in the literature [4–7], vibrational anharmonic resonances are less efficient in  $^{12}\text{C}_2\text{HD}$  than for other acetylene isotopologues and do not need to be included in the model, at least for lower energy bending states.

The present set of programs has a number of specific features favoring the search for new lines and bands from automatically generated predictions. As a result, we could slightly extend the previous literature analysis [2]. The full data set now amounts to 4514 vibration–rotation lines, with 4424 from Ref. [2] and 90 newly assigned lines. Most of these (85) arise from a new weak band, namely  $2v_4+v_5 \leftarrow 2v_4$  ( ${}^1\Pi \leftarrow \Delta$ ). The remaining new lines correspond to additional  $J$ -values in known branches. For completeness, we remind that the  $2v_4+v_5$  ( ${}^1\Pi$ ) state has already been characterized through the observation of the  $2v_4+v_5 \leftarrow v_4$  ( ${}^1\Pi \leftarrow \Pi$ ),  $2v_4+v_5 \leftarrow v_5$  ( ${}^1\Pi \leftarrow \Pi$ ) and  $2v_4+v_5 \leftarrow \text{G.S.}$  ( ${}^1\Pi \leftarrow \Sigma^+$ ) bands [2]. The status for the new or modified assignments is summarized in Table 3, while Table 4 lists the lines from the newly identified band. Fig. 3 and Table 5 provide an overview of the full data set used in the global fit.

A weighted least-squares fitting procedure was adopted, accounting for the experimental accuracy estimated to be  $5 \times 10^{-4} \text{ cm}^{-1}$ . As usual in such procedures, the selection of higher-order terms in the model is not unambiguous, given the high correlation between some of the parameters. We included only those higher-order constants that seemed most efficient in reducing the standard deviation of the fit, while keeping a reasonable value compared to the corresponding ones of lower order in the development.

The fitting procedure led to a set of 62 parameters listed in Table 6, with dimensionless standard deviation of 0.79 on 4347 fitted lines out of 4514 assigned transitions. A total of 167 lines presenting anomalously large (obs.–calc.) values were excluded from the fit. They correspond to very weak and/or blended lines. A comparison between the present results and those reported in Ref. [2] shows that the quality of the fit is very similar and that the corresponding parameters are in good agreement. Indeed, the presently adopted Hamiltonian and that in Ref. [2] only differ by the choice of some of the higher-order or interaction terms. Moreover, slightly different parameters and rejection limits for the exclusion of lines from the final fit have been selected in the two analyses.

**Table 2**Terms in the Hamiltonian used to perform the global vibration–rotation fit in  $^{12}\text{C}_2\text{HD}^a$ 

$$G_v^0 = \sum_{i=1,5} \tilde{\alpha}_i^0 v_i + \sum_{i \leq j} x_{ij}^0 v_i v_j + \sum_{b < b' = 4,5} x_{bb'}^0 l_b l_{b'} + \sum_{i \leq j < m} y_{ijm} v_i v_j v_m + \sum_{i,b < b'} y_{ibb'} v_i l_b l_{b'}$$

$$\langle l_4, l_5 | \hat{H} | l_4 \mp 2, l_5 \pm 2 \rangle = \frac{1}{4} r_{45} [(v_4 \pm l_4)(v_4 \mp l_4 + 2)(v_5 \mp l_5)(v_5 \pm l_5 + 2)]^{1/2}$$

$$r_{45} = r_{45}^0 + \sum_i r_{45,i} (v_i - \delta_{i4} - \delta_{i5}) + r_{45} J(J+1)$$

$$r_{45j} = r_{45j}^0 + \sum_i r_{45j,i} (v_i - \delta_{i4} - \delta_{i5})$$

$$E_{rv}^0 = G_v^0 + B_v [J(J+1) - k^2] - D_v [J(J+1) - k^2]^2 + H_v [J(J+1) - k^2]^3$$

$$B_v = B_0 - \sum_i \alpha_i^0 v_i + \sum_{i \leq j} \gamma_{ij}^0 v_i v_j + \sum_{b < b'} \gamma_{bb'}^0 l_b l_{b'} + \sum_{i \leq j < m} \varepsilon_{ijm} v_i v_j v_m + \sum_{i,b < b'} \varepsilon_{ibb'} v_i l_b l_{b'}$$

$$D_v = D_0 + \sum_i \beta_i^0 v_i$$

$$H_v = H_0$$

$$\langle l_b | H | l_b \pm 2 \rangle = \frac{1}{4} q_b [(v_b \mp l_b)(v_b \pm l_b + 2)]^{1/2} F_{\pm}(J, k) F_{\pm}(J, k \pm 1)$$

$$q_b = q_b^0 + \sum_i q_{bi} (v_i - \delta_{ib}) + \sum_{i \leq j} q_{b,ij} (v_i - \delta_{ib})(v_j - \delta_{jb}) + q_{bj} J(J+1)$$

$$q_{bj} = q_{bj}^0 + \sum_i q_{b,j,i} (v_i - \delta_{ib})$$

$$\langle l_b, l_{b'} | H | l_b \pm 4, l_{b'} \mp 2 \rangle = \frac{1}{8} q_{bb'b'} [(v_b \mp l_b)(v_b \pm l_b + 2)(v_b \mp l_b - 2)(v_b \pm l_b + 4)(v_{b'} \pm l_{b'}) (v_{b'} \mp l_{b'} + 2)]^{1/2} F_{\pm}(J, k)$$

$$\langle l_b | H | l_b \pm 4 \rangle = \frac{1}{4} u_{bb} [(v_b \mp l_b)(v_b \pm l_b + 2)(v_b \mp l_b - 2)(v_b \pm l_b + 4)]^{1/2} F_{\pm}(J, k) F_{\pm}(J, k \pm 1) F_{\pm}(J, k \pm 2) F_{\pm}(J, k \pm 3)$$

$$F_{\pm}(J, k) = [J(J+1) - k(k \pm 1)]^{1/2}$$

<sup>a</sup> In the terms,  $i, j, m, n$  refer to the five modes of vibration,  $b$  and  $b'$  specifically to the bending ones and  $k = l_4 + l_5$ . The notation  $\delta_{ij}$  is the usual notation for the delta of Kronecker function.

**Table 3**Bands of  $^{12}\text{C}_2\text{HD}$  in the bending region with additional assignments compared to the literature

Transition	Symmetry	$\nu_C^a$	Assigned transitions
$\nu_5 \leftarrow \text{G.S.}$	$\Pi \leftarrow \Sigma^+$	677.8077 <sup>b</sup>	$P_{e-e} (2-41); R_{e-e} (0-42); Q_{f-e} (1-42)$
$2\nu_5 \leftarrow \nu_5$	$\Sigma^+ \leftarrow \Pi$	664.4186 <sup>b</sup>	$P_{e-e} (1-34); R_{e-e} (1-35); Q_{e-f} (6-36)$
$3\nu_5 \leftarrow 2\nu_5$	$\Phi \leftarrow \Delta$	684.9650 <sup>b</sup>	$P_{f-f} (4-21); R_{f-f} (2-19); Q_{e-f} (3-22); Q_{f-e} (3-20); P_{e-e} (4-21); R_{e-e} (2-19)$
$2\nu_4 + \nu_5 \leftarrow 2\nu_4$	${}^1\Pi \leftarrow \Delta$	683.7504	$P_{e-e} (2-15); R_{e-e} (6-10); Q_{e-f} (3-21); Q_{f-e} (3-27); P_{f-f} (4-19); R_{f-f} (5-16)$

<sup>a</sup> The band center (in  $\text{cm}^{-1}$ ) is  $\nu_C = G_v^0 - B_v k^2 - D_v k^4 - (G_v^0 - B_v k'^2 - D_v k'^4)$ .

<sup>b</sup> Band previously reported in Ref. [2]. The range of the  $J$  values has been extended.

The resulting vibrational term values are provided in Table 7, for each  $k$ -sub-state. They correspond to calculated rotationless energies,  $G_C$  defined as

$$G_C = G_v^0 - B_v k'^2 - D_v k'^4 \quad (1)$$

with  $k = l_4 + l_5$ . Expressions for  $G_v^0$ ,  $B_v$  and  $D_v$  can be found in Table 2.

#### 4. Intensity simulations and line list

Assuming that a global ro-vibrational analysis has been previously performed on the experimental wavenumbers available, the automatic calculation of the relative intensities of all allowed transitions between two vibrational polyads in

**Table 4**List of the vibration–rotation lines of the  $2\nu_4+\nu_5\leftarrow 2\nu_4$  ( $^1\Pi\leftarrow\Delta$ ) band newly assigned in the spectrum of  $^{12}\text{C}_2\text{HD}$ 

$J$	$P_e$ ( $J$ ) ( $\text{cm}^{-1}$ )	Obs.–calc. ( $10^{-3}\text{cm}^{-1}$ )	$Q_r$ ( $J$ ) ( $\text{cm}^{-1}$ )	Obs.–calc. ( $10^{-3}\text{cm}^{-1}$ )	$R_e$ ( $J$ ) ( $\text{cm}^{-1}$ )	Obs.–calc. ( $10^{-3}\text{cm}^{-1}$ )
2	679.76212	0.19				
3	677.76478	0.27	683.73882	–0.09		
4	675.76492	0.17	683.73208	0.54		
5	673.76265	0.23	683.72248	–0.20		
6	671.75712	–0.12	683.71382	1.27	697.64531	–0.13
7	669.74895	0.09	683.70134	–0.10		
8	667.73661	–0.29	683.68970	0.04	701.59194	–0.24
9	665.72083	–0.11	683.67713	–0.45	703.55967	–0.51
10	663.70024	–0.29	683.66600	0.37	705.52377	–0.28
11	661.67508	–0.11	683.65410	–0.15		
12	659.64442	–0.04	683.64393	0.00		
13	657.60782	–0.07	683.63542	0.20		
14	655.56507	–0.02	683.62746	–1.20		
15	653.51560	–0.12	683.62336	–1.50		
16			683.62336	–1.05		
17			683.62746	–0.48		
18			683.63542	–0.67		
19			683.64932	–0.14		
21			683.69483	0.56		

$J$	$P_f$ ( $J$ ) ( $\text{cm}^{-1}$ )	Obs.–calc. ( $10^{-3}\text{cm}^{-1}$ )	$Q_e$ ( $J$ ) ( $\text{cm}^{-1}$ )	Obs.–calc. ( $10^{-3}\text{cm}^{-1}$ )	$R_f$ ( $J$ ) ( $\text{cm}^{-1}$ )	Obs.–calc. ( $10^{-3}\text{cm}^{-1}$ )
3			683.79199	–1.89		
4	675.82157	–0.16	683.82213	–0.37		
5	673.85823	–0.17	683.85777	–0.10	695.86500	–0.17
6	671.90292	–0.06	683.89963	–0.10		
7	669.95577	0.04	683.94785	0.08	699.96612	–0.04
8	668.01738	0.42	684.00153	–0.09	702.02943	–0.17
9	666.08699	–0.04	684.06054	–0.34	704.10182	–0.35
10	664.16634	0.01	684.12512	0.00	706.18421	–0.10
11	662.25555	0.23	684.19380	–0.06	708.27624	–0.21
12	660.35411	–0.35	684.26647	–0.19	710.37890	–0.19
13	658.46396	–0.33	684.34298	–0.07	712.49285	0.09
14	656.58529	–0.04	684.42224	–0.39	714.61794	–0.04
15	654.71827	0.10	684.50487	–0.17	716.75586	0.56
16			684.58989	–0.10	718.90467	–0.60
17	651.02189	0.27	684.67719	–0.11		
18			684.76680	–0.07		
19	647.37994	0.45	684.85868	–0.06		
20			684.95303	0.00		
21			685.04923	–0.73		
22			685.14963	–0.21		
23			685.25263	–0.40		
24			685.35976	–0.18		
25			685.47074	–0.24		
27			685.70587	–1.32		

the electronic ground state of a linear molecule is made possible by the program package developed in Louvain-La-Neuve. The general procedure to calculate relative intensities of linear molecule spectra is detailed in Ref. [19].

Briefly, for a given spectrum recorded at a temperature  $T$ , the relative intensity of a transition is given by

$$S_{\text{rel}} = C \nu g e^{-(E'/kT)} (1 - e^{-(\nu/kT)}) |R|^2 \quad (2)$$

with  $C$  a factor depending on the experimental conditions,  $\nu$  the wavenumber of the transition,  $g$  the nuclear spin statistical weight of the lower state and  $R$  the effective transition moment. The other terms are the Boltzmann factor and the stimulated emission factor, which is important for lower-frequency transitions.

The calculation of spectra with intensities is fully automatic. The maximum energy for the lower states to be considered for hot band contribution is defined by the user. The value of the transition moment is also imposed by the user, associated with the selection rule, which sets the upper states to be considered. All transitions with intensity above a selected threshold are considered in the spectrum calculated using Eq. (2).

A list of lines with their position and relative intensity has been generated for all the bands in the range  $450\text{--}800\text{cm}^{-1}$ , thus around the  $\nu_4$  and  $\nu_5$  cold bands. Absolute intensities for each line have been calculated using the measured absolute

**Table 5**Summary of the full data set used in the global vibration–rotation fit of the bending states in  $^{12}\text{C}_2\text{HD}^a$ 

Upper state				Lower state				Lines	$J_{\min}$	$J_{\max}$	Ref.
$v_4$	$v_5$	$l_4$	$l_5$ e/f	$v_4$	$v_5$	$l_4$	$l_5$ e/f				
1	0	1	0e	0	0	0	0e	63	1	33	a
1	0	1	0f	0	0	0	0e	40	2	41	a
0	1	0	1e	0	0	0	0e	83	1	43	b
0	1	0	1f	0	0	0	0e	42	1	42	a
2	0	0	0e	1	0	1	0e	59	0	31	a
2	0	0	0e	1	0	1	0f	21	9	29	a
2	0	2	0e	1	0	1	0e	42	2	25	a
2	0	2	0e	1	0	1	0f	30	5	34	a
2	0	2	0f	1	0	1	0f	56	2	30	a
2	0	2	0f	1	0	1	0e	34	3	36	a
1	1	1	-1e	1	0	1	0e	54	0	28	a
1	1	1	-1e	1	0	1	0f	35	3	37	a
1	1	1	-1f	1	0	1	0f	69	0	37	a
1	1	1	-1f	1	0	1	0e	26	1	27	a
1	1	1	1e	1	0	1	0e	68	2	37	a
1	1	1	1e	1	0	1	0f	29	2	30	a
1	1	1	1f	1	0	1	0f	49	2	28	a
1	1	1	1f	1	0	1	0e	35	2	37	a
1	1	1	-1e	0	1	0	1e	35	2	21	a
1	1	1	-1e	0	1	0	1f	26	1	27	a
1	1	1	-1f	0	1	0	1f	30	4	21	a
1	1	1	-1f	0	1	0	1e	21	1	24	a
1	1	1	1e	0	1	0	1e	47	2	30	a
1	1	1	1e	0	1	0	1f	17	2	20	a
1	1	1	1f	0	1	0	1f	48	2	30	a
1	1	1	1f	0	1	0	1e	15	4	19	a
0	2	0	0e	0	1	0	1e	69	0	36	a
0	2	0	0e	0	1	0	1f	28	6	36	b
0	2	0	2e	0	1	0	1e	63	2	35	a
0	2	0	2e	0	1	0	1f	24	2	25	a
0	2	0	2f	0	1	0	1f	61	2	34	a
0	2	0	2f	0	1	0	1e	34	2	35	a
2	1	0	1e	2	0	0	0e	47	1	24	a
2	1	0	1f	2	0	0	0e	29	1	29	a
2	1	2	1e	2	0	2	0e	44	3	28	a
2	1	2	1f	2	0	2	0e	26	3	28	a
2	1	2	1f	2	0	2	0f	47	3	30	a
2	1	2	1e	2	0	2	0f	20	3	22	a
1	2	1	0f	1	1	1	-1e	19	1	22	a
1	2	-1	2e	1	1	1	-1e	44	1	23	a
1	2	-1	2f	1	1	1	-1e	24	3	28	a
1	2	1	0f	1	1	1	-1f	37	1	23	a
1	2	1	0e	1	1	1	-1f	12	12	23	a
1	2	-1	2f	1	1	1	-1f	35	1	18	a
1	2	-1	2e	1	1	1	-1f	22	6	27	a
1	2	1	0e	1	1	1	1e	37	1	22	a
1	2	1	0f	1	1	1	1e	11	5	15	a
1	2	1	0f	1	1	1	1f	29	1	18	a
1	2	1	0e	1	1	1	1f	12	4	15	a
1	2	1	2e	1	1	1	1e	40	3	23	a
1	2	1	2f	1	1	1	1e	17	3	26	a
1	2	1	2f	1	1	1	1f	44	3	29	a
1	2	1	2e	1	1	1	1f	20	3	28	a
0	3	0	1e	0	2	0	0e	40	1	25	a
0	3	0	1f	0	2	0	0e	25	1	25	a
0	3	0	3e	0	2	0	2f	20	3	22	b
0	3	0	3e	0	2	0	2e	36	3	20	a
0	3	0	3f	0	2	0	2e	18	3	20	a
0	3	0	3f	0	2	0	2f	36	3	20	a
2	0	0	0e	0	0	0	0e	90	0	45	a
2	0	2	0e	0	0	0	0e	76	5	43	a
1	1	1	-1e	0	0	0	0e	87	0	44	a
1	1	1	1e	0	0	0	0e	71	5	43	a
0	2	0	0e	0	0	0	0e	96	0	49	a
0	2	0	2e	0	0	0	0e	63	8	44	a
3	0	1	0e	1	0	1	0e	78	1	40	a
3	0	1	0f	1	0	1	0f	75	1	39	a

Table 5 (continued)

Upper state				Lower state				Lines	$J_{\min}$	$J_{\max}$	Ref.
$v_4$	$v_5$	$l_4$	$l_5$ e/f	$v_4$	$v_5$	$l_4$	$l_5$ e/f				
2	1	0	1e	1	0	1	0e	65	1	34	a
2	1	0	1f	1	0	1	0f	33	1	17	a
2	1	2	-1e	1	0	1	0e	71	1	37	a
2	1	2	-1f	1	0	1	0f	76	1	40	a
2	1	2	-1f	1	0	1	0e	13	1	13	a
2	1	2	-1e	2	0	2	0e	18	1	14	b
2	1	2	-1e	2	0	2	0f	18	3	21	b
2	1	2	-1f	2	0	2	0e	24	3	27	b
2	1	2	-1f	2	0	2	0f	25	3	18	b
2	1	0	1e	0	1	0	1e	61	1	33	a
2	1	0	1f	0	1	0	1f	68	1	37	a
2	1	0	1f	0	1	0	1e	14	1	14	a
2	1	0	1e	0	1	0	1f	11	1	11	a
2	1	2	-1e	0	1	0	1e	46	1	25	a
2	1	2	-1f	0	1	0	1f	56	1	32	a
1	2	1	0e	1	0	1	0e	81	1	42	a
1	2	1	0f	1	0	1	0f	80	1	41	a
1	2	1	0f	1	0	1	0e	18	1	18	a
1	2	1	0e	1	0	1	0f	9	7	15	a
1	2	-1	2e	1	0	1	0e	43	1	27	a
1	2	-1	2f	1	0	1	0f	63	1	36	a
1	2	1	0e	0	1	0	1e	61	1	34	a
1	2	1	0f	0	1	0	1f	52	1	27	a
1	2	-1	2e	0	1	0	1e	69	1	36	a
1	2	-1	2f	0	1	0	1f	67	1	36	a
1	2	-1	2f	0	1	0	1e	9	1	9	a
1	2	-1	2e	0	1	0	1f	8	1	10	a
0	3	0	1e	0	1	0	1e	80	1	42	a
0	3	0	1e	0	1	0	1f	13	1	15	a
0	3	0	1f	0	1	0	1f	79	1	42	a
0	3	0	1f	0	1	0	1e	15	1	16	a
3	0	1	0e	0	0	0	0e	39	2	23	a
3	0	1	0f	0	0	0	0e	22	1	22	a
2	1	0	1e	0	0	0	0e	38	1	21	a
2	1	0	1f	0	0	0	0e	23	1	23	a
2	1	2	-1e	0	0	0	0e	52	1	28	a
2	1	2	-1f	0	0	0	0e	24	1	24	a
1	2	-1	2e	0	0	0	0e	48	1	27	a
1	2	-1	2f	0	0	0	0e	27	4	30	a
0	3	0	1e	0	0	0	0e	62	1	33	a
0	3	0	1f	0	0	0	0e	34	1	34	a

<sup>a</sup> All labels are identified in the text. Ref. a is Fusina et al. [2]. Ref. b is the present work.

band intensities and the predicted relative line intensities so that the sum of all the lines belonging to each cold band and to related overlapping hot bands equals the measured band intensity.

Using this line list, a model spectrum was calculated, as shown in Fig. 2 for  $v_5$ . The comparison between the model and the experiment is very good, including the three strongest hot band features in the spectral range presented. One feature appearing at  $674.3 \text{ cm}^{-1}$  in the experimental spectra recorded at higher pressure (not shown) corresponds to the Q branch of  $v_5$  for  $^{13}\text{CH}^{12}\text{CD}$  (band origin at  $674.169 \text{ cm}^{-1}$ ) [20]. The corresponding Q branch for  $^{12}\text{CH}^{13}\text{CD}$ , expected to be present in the sample with similar abundance as  $^{13}\text{CH}^{12}\text{CD}$ , is at  $677.867 \text{ cm}^{-1}$  and therefore buried under the strong feature of  $^{12}\text{C}_2\text{HD}$ . Another example, the fundamental bending transition  $v_4 \leftarrow \text{GS}$ , experimental and simulated, is shown in Fig. 4.

The line list is available from the authors and will be soon incorporated in the next release of the GEISA database.

## 5. Conclusions

The integrated intensities of all fundamental bands and of two overtone and three combination bands observed in the range  $25\text{--}2.5 \mu\text{m}$  have been measured in  $^{12}\text{C}_2\text{HD}$ , with improved accuracy compared to the literature results. We have also extended a previous vibration–rotation analysis in the bending range, identifying for the first time the  $2v_4+v_5 \leftarrow 2v_4$  ( $^1I \leftarrow \Delta$ ) weak band. All 4347 assigned vibration–rotation lines were fitted to a set of 62 parameters of a global

**Table 6**Vibration–rotation parameters in  $^{12}\text{C}_2\text{HD}$  ( $\text{cm}^{-1}$ )<sup>a</sup>

om4	517.40964(69)		D0	1.133472(10)	E–06
om5	676.187802(67)		beta4	3.5107(47)	E–08
x44	–0.15045(50)		beta5	1.4770(28)	E–08
x45	0.70685(11)		H0	0.437(36)	E–12
x55	–2.598026(64)		q4	–4.437867(85)	E–03
xl4l4	2.11030(54)		q4v4	–0.03857(36)	E–03
xl4l5	0.85218(10)		q4v5	0.00364(11)	E–03
xl5l5	5.161678(51)		q4v44	–0.128(16)	E–05
y444	–0.035273(81)		q4v45	0.260(22)	E–05
y445	0.042155(47)		q4J	3.7980(90)	E–08
y455	0.043197(29)		q4Jv4	0.1190(89)	E–08
y555	0.030397(16)		q5	–3.525776(69)	E–03
y4l4l4	0.04136(26)		q5v4	–0.01441(29)	E–03
y4l4l5	–0.103146(72)		q5v5	–0.05509(53)	E–03
y4l5l5	0.020610(66)		q5v44	0.171(23)	E–05
y5l4l4	0.04179(11)		q5v45	–0.238(24)	E–05
y5l4l5	–0.048770(47)		q5v55	0.354(25)	E–05
y5l5l5	0.018975(18)		q5J	2.1804(53)	E–08
BO	991.527807(10)	E–03	q5Jv5	0.0690(70)	E–08
alpha4	–2.64343(35)	E–03	q445	–0.350(11)	E–05
alpha5	–1.47980(17)	E–03	q455	0.1226(75)	E–05
gam44	3.156(12)	E–05	u44	–0.1535(68)	E–08
gam45	–2.586(12)	E–05	u55	–0.1000(39)	E–08
gam55	2.528(14)	E–05	r45	2.167573(31)	
gl4l4	–8.078(38)	E–05	r45v4	0.23388(23)	
gl5l5	–11.796(18)	E–05	r45v5	0.07509(40)	
eps445	0.1986(74)	E–05	r45J	–2.4522(91)	E–05
eps555	–0.0459(39)	E–05	r45Jv4	0.060(19)	E–05
eps4l44	–0.090(15)	E–05	r45Jv5	–0.555(24)	E–05
eps4l45	0.1019(93)	E–05			
eps5l44	–0.222(12)	E–05			
eps5l45	0.1939(72)	E–05			
eps5l55	–0.2374(70)	E–05			

<sup>a</sup> The standard deviation ( $1\sigma$ ) is indicated in parentheses, in the units of the last quoted digit. The parameters are labeled in agreement with the model defined in Table 2.

**Table 7**Vibrational term values  $G_c$  ( $\text{cm}^{-1}$ ) of all observed  $\nu_i$  bending sublevels in  $^{12}\text{C}_2\text{HD}$ 

$\nu_1$	$\nu_2$	$\nu_3$	$\nu_4$	$\nu_5$	$l_4$	$l_5$	$e/f$	$k$	$G_c$ ( $\text{cm}^{-1}$ )
0	0	0	0	0	0	0	<i>e</i>	0	0.000
0	0	0	1	0	1	0	<i>a</i>	1	518.381
0	0	0	0	1	0	1	<i>a</i>	1	677.808
0	0	0	2	0	0	0	<i>e</i>	0	1033.936
0	0	0	2	0	2	0	<i>a</i>	2	1038.721
0	0	0	1	1	1	1	<i>a</i>	2	1195.749
0	0	0	1	1	1	–1	<i>f</i>	0	1196.163
0	0	0	1	1	1	–1	<i>e</i>	0	1200.498
0	0	0	0	2	0	0	<i>e</i>	0	1342.227
0	0	0	0	2	0	2	<i>a</i>	2	1359.049
0	0	0	3	0	1	0	<i>a</i>	1	1551.158
0	0	0	3	0	3	0	<i>a</i>	3	1561.041
0	0	0	2	1	0	1	<i>a</i>	1	1712.170
0	0	0	2	1	2	1	<i>a</i>	3	1715.598
0	0	0	2	1	2	–1	<i>a</i>	1	1722.471
0	0	0	1	2	1	0	<i>a</i>	1	1861.859
0	0	0	1	2	1	2	<i>a</i>	3	1876.571
0	0	0	1	2	–1	2	<i>a</i>	1	1882.439
0	0	0	0	3	0	1	<i>a</i>	1	2010.225
0	0	0	0	3	0	3	<i>a</i>	3	2044.014

<sup>a</sup> Identical value for *e* and *f* components.

Hamiltonian. The dimensionless standard deviation of the fit is equal to 0.79. These line position and line intensity results were used to simulate the spectrum. The focus was set on the bending range, of planetary and astrophysical relevance. A related line list was produced, to be delivered to databases.

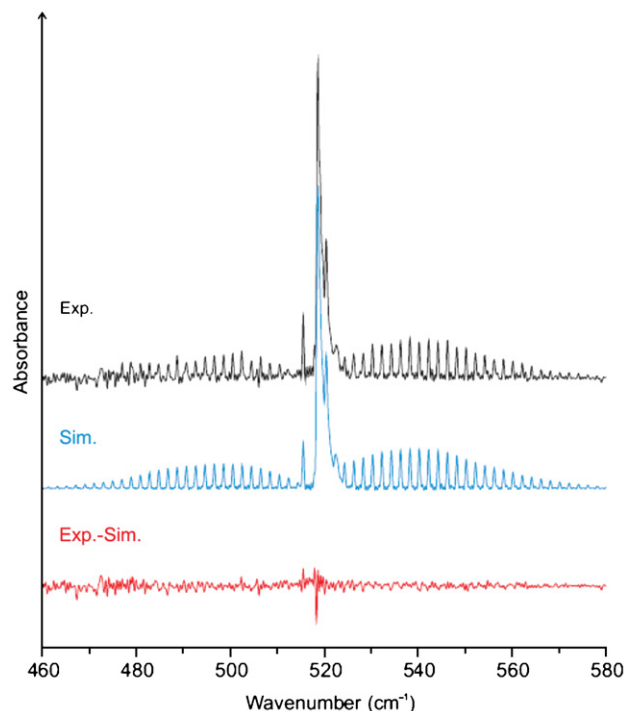


Fig. 4. Comparison between simulated and experimental spectra near the  $\nu_4$  bending of  $^{12}\text{C}_2\text{HD}$  ( $T = 296\text{ K}$ , pathlength = 10.6 m,  $P = 0.0245\text{ mbar}$ , resolution =  $0.5\text{ cm}^{-1}$ ).

## Acknowledgments

This work was sponsored, in Italy, by the Università di Bologna and MIUR (PRIN “Dinamiche molecolari”) and, in Belgium, by the Fonds National de la Recherche Scientifique (FNRS, contracts FRFC and IISN) and the “Action de Recherches Concertées de la Communauté française de Belgique”. It is performed within the “LEA HiRes “collaboration between ULB and UCL. S.R. thanks FRIA for financial support and the “Communauté française de Belgique” for a grant to travel to Bologna. We thank Dr. J. Vander Auwera (ULB) for useful discussions.

## References

- [1] Coustenis A, Jennings DJ, Jolly A, Bénilan Y, Nixon CA, Vinatier S, et al. Detection of  $\text{C}_2\text{HD}$  and the D/H ratio on Titan. *Icarus* 2008;197:539–48.
- [2] Fusina L, Cané E, Tamassia F, Di Lonardo G. The infrared spectrum of  $^{12}\text{C}_2\text{HD}$ : the bending states up to  $\nu_4+\nu_5 = 3$ . *Mol. Phys.* 2005;103:3263–70.
- [3] Cazzoli G, Puzzarini C, Fusina L, Tamassia F. Rotational spectra of deuterated acetylenes:  $\text{DCCH}$ ,  $\text{D}^{13}\text{CCH}$  and  $\text{DC}^{13}\text{CH}$ . *J. Mol. Spectrosc.* 2008;247:115–8.
- [4] Liévin J, Abbouti Tamsamani M, Gaspard P, Herman M. Overtone spectroscopy and dynamics in monodeuteroacetylene ( $\text{C}_2\text{HD}$ ). *Chem. Phys.* 1995;190:419–45.
- [5] Abbouti Tamsamani M, Herman M. Anharmonic resonances in monodeuteroacetylene ( $^{12}\text{C}_2\text{HD}$ ). *Chem. Phys. Lett.* 1996;260:253–6.
- [6] Abbouti Tamsamani M, Herman M. Anharmonic resonances in monodeuteroacetylene ( $^{12}\text{C}_2\text{HD}$ ). *Chem. Phys. Lett.* Erratum 1997;264:556.
- [7] Herman M, Depiesse C, Di Lonardo G, Fayt A, Fusina L, Hurtmans D, et al. The vibration–rotation spectrum of  $^{12}\text{C}_2\text{HD}$ : new overtone bands and global vibrational analysis. *J. Mol. Spectrosc.* 2004;228:499–510.
- [8] Fusina L, Tamassia F, Di Lonardo G. The infrared spectrum of  $^{12}\text{C}_2\text{HD}$ : the stretching–bending combination bands in the  $1800\text{--}4700\text{ cm}^{-1}$  region. *Mol. Phys.* 2005;103:2613–20.
- [9] Eggers DF, Hisatsune Jr. IC, Van Alten L. Bond moments, their reliability and additivity: sulfur dioxide and acetylene. *J. Phys. Chem.* 1955;59(11):1124–9.
- [10] Kim K, King WT. Integrated infrared intensities in  $\text{HCCH}$ ,  $\text{DCCD}$  and  $\text{HCCD}$ . *J. Mol. Struct.* 1979;57:201–7.
- [11] Fayt A, Robert S, Di Lonardo G, Fusina L, Tamassia F, Herman M. Vibration–rotation energy pattern in acetylene:  $^{13}\text{CH}^{12}\text{CH}$  up to  $6750\text{ cm}^{-1}$ . *J. Chem. Phys.* 2007;126. 114303/1–114303/8.
- [12] Kabbadj Y, Herman M, Di Lonardo G, Fusina L, Johns JWC. The bending energy levels of acetylene. *J. Mol. Spectrosc.* 1991;150:535–65.
- [13] Robert S, Herman M, Vander Auwera J, Di Lonardo G, Fusina L, Blanquet G, et al. The bending vibrations in  $^{12}\text{C}_2\text{H}_2$ : global vibration–rotation analysis. *Mol. Phys.* 2007;105:559–68.
- [14] Huet TR, Herman M, Johns JWC. The bending vibrational levels in acetylene- $\text{d}_2$  ( $\text{C}_2\text{D}_2$  ( $X^1\Sigma_g^+$ )). *J. Chem. Phys.* 1991;94:3407–14.
- [15] Cané E, Cazzoli G, Di Lonardo G, Dore L, Escribano R, Fusina L. The infrared spectrum of  $^{13}\text{C}_2\text{D}_2$ : the bending states up to  $\nu_4+\nu_5 = 2$ . *J. Mol. Spectrosc.* 2002;216:447–53.
- [16] Di Lonardo G, Baldan A, Bramati G, Fusina L. The infrared spectrum of  $^{12}\text{C}^{13}\text{CH}_2$ : the bending states up to  $\nu_4+\nu_5 = 4$ . *J. Mol. Spectrosc.* 2002;213:57–63.

- [17] Vigouroux C, Fayt A, Guarnieri A, Huckauf A, Bürger H, Lentz D, et al. Global rovibrational analysis of HCCNC based on infrared and millimeter-wave spectra. *J. Mol. Spectrosc.* 2000;202:1–18.
- [18] Fayt A, Vigouroux C, Willaert F, Margules L, Constantin LF, Demaison J, et al. Global analysis of high resolution infrared and rotational spectra of HCCC<sup>15</sup>N up to 1335 cm<sup>-1</sup>. *J. Mol. Struct.* 2004;695–696:295–311.
- [19] Fayt A, Vigouroux C, Winther F. Analysis of the  $\nu_9$  band complex of dicyanoacetylene and application of a theory of relative intensities to all subbands. *J. Mol. Spectrosc.* 2004;224:114–30.
- [20] Fusina L, Cané E, Tamassia F, Di Lonardo G. High-resolution infrared spectroscopy of H<sup>12</sup>C<sup>13</sup>CD and H<sup>13</sup>C<sup>12</sup>CD in the 470–5200 cm<sup>-1</sup> spectral region. *Mol. Phys.* 2007;105:2321–5.